

Manipulated wettability of a superhydrophobic quartz crystal microbalance through electrowetting

K. D. Esmeryan¹, G. McHale², C. L. Trabi², N. R. Galdi³ and M. I. Newton³

¹Georgi Nadjakov Institute of Solid State Physics, 72, Tzarigradsko Chaussee Blvd., 1784 Sofia

²Faculty of Engineering and Environment, Northumbria University, Ellison Place, Newcastle upon Tyne, NE1 8ST, UK

³School of Science and Technology, Nottingham Trent University, Clifton Lane, Nottingham, NG11 8NS, UK

Abstract:

The liquid phase response of quartz crystal microbalances (QCM) with a thin coating ($\sim 9 \mu\text{m}$) of epoxy resin with and without a carbon nanoparticles top layer is reported. The nanoparticles convert the epoxy surface to a superhydrophobic one with a high static contact angle ($\sim 151^\circ$ - 155°) and low contact angle hysteresis ($\sim 1^\circ$ - 3.7°) where droplets of water are in the suspended Cassie-Baxter state. The frequency decrease of the fully immersed QCM with the superhydrophobic surface is less than with only epoxy layer, thus indicating a decoupling of the QCM response. A wettability transition to a liquid penetrating into the surface roughness state (for droplets a high contact angle hysteresis Wenzel state) was triggered using a molarity of ethanol droplet test (MED) and electrowetting; the MED approach caused some surface damage. The electrowetting induced transition caused a frequency decrease of 739 Hz at a critical voltage of ~ 100 V compared to the QCM in air. This critical voltage correlates to a contact angle decrease of 26° and a high contact angle hysteresis state in droplet experiments. These experiments provide a proof-of-concept that QCMs can be used to sense wetting state transitions and not only mass attachments or changes in viscosity-density products of liquids.

PACS:

68.08Bc – wetting in liquid solid interfaces

77.65Fs – quartz crystal resonators

Keywords: Superhydrophobic, quartz crystal microbalance, epoxy resin, carbon nanoparticles, electrowetting.

1. Introduction

Quartz Crystal Microbalances (QCM) provide a simple and effective method to detect changes of physical properties of thin films adhering to their surfaces. Sauerbrey first discovered that a film deposited to the surface of a piezoelectric quartz crystal resonator will cause a decrease in the resonance frequency proportional to the mass per unit area of the film attached [1]. The Sauerbrey equation is valid under the condition that the film is thin, smooth and rigidly coupled to the oscillatory motion of the crystal surface.

In 1982 Nomura and Okuhara showed that the QCM can oscillate in, and detect properties of, a liquid environment [2]. Its utility as a liquid phase sensor has been demonstrated for many applications in electrochemistry [3] and immunology [4]. When the crystal surface is brought into a contact with a liquid, a viscous entrainment of liquid near the surface occurs due to the acoustic wave, thus causing both a frequency decrease and an energy loss depending on the viscosity-density product of the liquid [5,6]. This phenomenon is described by the Kanazawa and Gordon equation and it is valid under a no slip boundary condition, which implies that the velocity of displacement of the quartz substrate and the liquid at the solid-liquid interface match. However if the crystal surface has an appropriate hydrophobic chemistry and consist of high aspect ratio surface roughnesses, the effect of hydrophobicity will be amplified to superhydrophobicity (SH) [7]. When such a solid surface has a protrusions, which are tall enough and sufficiently close water does not penetrate between them. In this situation the droplets ball up and are effectively suspended on the tips of the surface features. Moreover due to the small number of contact points with the solid they become extremely mobile and roll off easily. This type of surface is often called “slippy” and is described by the Cassie-Baxter equation [8]. If sufficient pressure is applied water will penetrate into the gaps between surface features and will contact the solid surface everywhere including the bottom part of the surface structure and up the sides and across the tops of the surface features. A droplet may still ball up but it will become immobile and unable to roll. The surface is said to be “sticky” and is described by the Wenzel equation [8]. Liquid phase QCMs sense interactions via the liquid close to the QCM surface within the shear wave penetration depth $\delta = (\eta/\pi f \rho)^{1/2}$ (1), where f is the resonance frequency of the crystal and η is the viscosity of the liquid. For a 5 MHz device immersed in water $\delta \sim 250$ nm. According to the considerations above it can be expected that the sensor response of QCM operating in a liquid environment will depend on the wetting state, Cassie-Baxter or Wenzel, of the quartz surface and should be able to detect wetting transitions between these two states. Recently has been reported that through a superhydrophobization of the QCM’s surface it is possible to decouple the sensor response [9-12].

In this paper we consider whether a sensor can be designed such that a small change in hydrophobicity triggers a complete switching of the wetting state; an idea speculated upon but not previously reported [13]. In principle, such a change could be due to the attachment of specific molecules, but the detection would not depend on the detectability of the mass change, but would be via their effect on the wetting state. To study the QCM response to a change in the wetting state of a superhydrophobic surface several other trigger mechanisms are possible including temperature, surface tension, mechanical, optical and magnetic changes or applied voltage via an electrowetting effect [14-16]. The two mechanisms studied in this paper are a surface tension induced switching using increasing concentrations of ethanol (molarity-of-ethanol droplet (MED) test) and electrowetting. Electrowetting involves application of electrical potential across liquid/dielectric/electrode sandwich structure to charge the solid-liquid interface. For a droplet the charge induced imbalance of forces near the liquid/dielectric contact line results in a decrease in the observed liquid contact angle [17]; on a superhydrophobic surface the electrocapillary pressure can cause a switch from the Cassie-Baxter suspended state to a Wenzel penetrating state [18].

In section 2, we first review the results of a model of QCM liquid response under the assumption of a no slip boundary condition and confirm that our experimental set up can provide results for glycerol/water solutions consistent with the Kanazawa and Gordon equation. We then describe a new method to create a superhydrophobic surface using an epoxy resin-soot composite surface coating; the

advantage of this surface coating is its ability to simultaneously act as the dielectric insulator for electrowetting. We also describe how MED tests can be used to switch wetting states and we characterize droplet contact angle changes for both the electrowetting and MED switching methods. In section 3, we investigate the possible relationship between QCM response and the wetting state transition of the superhydrophobic QCM device triggered by using MED tests and electrowetting.

2. Experimental set up

2.1. Calibration of the QCM

The liquid phase sensor response of QCM, which operates in a liquid environment, is usually expressed as proportional to the square root of the viscosity-density product of the liquid according to the Kanazawa and Gordon equation [5]. In our work, gold electrode quartz crystals with a fundamental frequency of 5 MHz and diameter of 25 mm were used, with frequency spectra being monitored using an Agilent Technologies 8712ET network analyzer over the range of 5.01-5.02 MHz. Resonance characteristics were measured at room temperature for crystal in air and in aqueous glycerol solutions with concentrations in the range of 0 ÷ 90 % per weight and fitted to a Butterworth-van-Dyke (BVD) model using LabView 10.1. A brief description of the BVD model is available in [9].

2.2. Decoupling of the sensor response of the QCM

It is expected that a superhydrophobic QCM surface could efficiently decouple its sensor response [9,19]. If this occurs, the crystal resonance spectra of the device should become relatively less sensitive to the viscous properties of the liquid. Thus both the resonance frequency decrease and bandwidth increase would be lower than that predicted by Kanazawa and Gordon. Many strategies to create superhydrophobic surfaces have been put forward including wax solidification, lithography, vapor deposition, template methods, polymer reformation, sublimation, plasma, electro spinning, sol-gel processing, electrochemical methods, hydrothermal synthesis, layer-by-layer deposition and one pot reactions [20]. Each method has particular advantages and disadvantages e.g. multistep procedures and harsh conditions, requirement of specialized reagents and equipment, durability and robustness of coating or applicability only to small areas of flat surfaces or specific materials [21]. The method we developed, suitable for our intended application, was based on the incomplete combustion of carbon nanoparticles (CNP) contained in a rapeseed oil mixture [22] or in candle soot [23] deposited on an epoxy coating layer. The method is facile and time efficient and did not require specialized equipments, dangerous reagents or complex process control. In previous use of the soot approach, the main drawback is the fragility of the structure because the particle-particle interactions are only physical and weak. Therefore when a droplet of water rolls off the surface, the drop carries soot particles with it until almost all of the soot deposit is removed and the drop undergoes a wetting transition. Increase in the structural robustness has previously been achieved by the development of a composite soot-polydimethylsiloxane (PDMS) based layer [24]. However for our QCM application PDMS, which belongs to the family of rubbery polymers [25], could complicate the QCM response reducing the quality of resonance and rigid response interpretation. Moreover, PDMS does not easily adhere to gold surfaces so an additional thin adhesive layer would be required. We therefore modified the superhydrophobic coating approach to use a soot-epoxy resin

composite layer. The liquid epoxy resin is transparent, rigid and has good surface adhesion and low viscosity, which allows a spin coating deposition technique, and thus the opportunity to form very thin rigid layers. The fully cured epoxy resin is rigid so the QCM can be expected to have low damping and higher operational frequency compared to using PDMS.

2.2.1. Epoxy resin preparation and spin coating deposition.

MAS epoxy resin with slow hardener in a ratio 2:1 was mixed for 2 minutes. After mixing, the prepared solution with viscosity $\eta_e=600$ cps was placed in a vacuum oven for 30 minutes to extract any air. The oven was set up to maintain a maximal pressure of 0.1 MPa and constant temperature of 21 °C. Then the quartz crystals were mounted one at the time in an Emhart spin coater and liquid epoxy resin was deposited from pipette onto their surfaces. The spin coating procedure was conducted with a spin velocity of 5000 rpm and spin duration of 50 seconds. The thickness of the layer achieved with these working parameters was $\sim (9\pm 0.5)$ μm .

2.2.2. Fabrication of epoxy resin-soot composite SH QCM

After spin coating deposition of the epoxy resin, the process parameters required to create a superhydrophobic crystal surface were determined. First a few soot coated SH glass slides were prepared exposing them over a flame of a burning wick, immersed in a rapeseed oil [22]. Then to achieve uniform and homogenous SH surfaces the soot coated glass slides were binded with the precured epoxy coated quartz crystals [24]. Since the viscosity of the epoxy resin is highly temperature and time sensitive [26] it was very important to find the best precuring time prior to soot deposition that resulted in a non-engulfed, but attached, soot layer. It was found that the optimal precuring time in a room temperature is 4 h and 20 minutes. For a complete and uniform transfer an additional mechanical force is required by pressing a finger on the glass slides. Eventually the soot coated glass samples were carefully peeled off from the epoxy resin coated QCMs and the quartz crystal patterns were held in a room temperature conditions until full cure is reached. For the used resin the full curing time is approximately 11 hours. The process was repeated for five from seven available QCMs. The other two QCMs, one with an uncoated surface and the other with an epoxy coated surface were used as reference devices. After full cure of the epoxy resin-soot coated QCM we verified the wettability of surfaces using static contact angle (SCA) and contact angle hysteresis (CAH) measurements for droplets of water. These were found to be in the range of 151°-155° and 1°-3.7°, respectively, thereby confirming a superhydrophobic surface with mobile droplet behavior [27].

2.3. Investigation and control of the wetting state transition of a SH QCM

When the superhydrophobic QCMs had been obtained we investigated the triggering of the wetting state transition and its detection by variations in the resonance frequency response and/or the dissipation factor. The first triggering mechanism which was used was based on surface tension changes using ethanol-water solutions with different concentrations. The molarity of ethanol droplet (MED), which sometimes is referred as critical surface tension or % ethanol test is widely applied to determine the level of water repellency for soils and other porous and granular patterns [28]. Drops of aqueous ethanol solutions with decreasing surface tension are placed on to different areas of the sample surface until a solution with sufficiently low surface tension is reached that just allows the drops to penetrate in. The % ethanol concentration at which the drops penetrate the porous surface is then taken to characterize the

level of hydrophobicity of the surface. In our case we investigated the wettability of SH QCM with increasing concentrations of ethanol-water solutions. First a 5 MHz gold electrode quartz crystal with diameter of 25 mm and uncoated surface was used as a reference device with aim to verify the QCM's response in aqueous ethanol solutions. Its frequency spectra were monitored using an Agilent technologies 8712ET network analyzer over the range of 5.018÷5.02 MHz. The sensor response was measured at room temperature for QCM in air and in ethanol solutions in concentration range of 0÷90 % per weight and then fitted to a BVD model using LabView 10.1. Subsequently a SH quartz crystal was tested for lower concentration range of 0÷12.5 % per weight and again fitted to the BVD model. By analyzing the resonance frequency shifts for both sets it was possible to assess whether the QCM is capable to detect the wetting state transition.

Four further SH QCMs with resonance frequency of 5 MHz were used and their wettability was manipulated through electrowetting. An epoxy coated QCM was used as a reference device in order to evaluate whether the observed frequency shifts were caused by a wetting state transition or by e.g. change in the piezoelectric stiffness of the crystal. A 30 MHz synthesized function generator DS345 was connected via coaxial cable to the input of a voltage amplifier TREK PZD700A and used to set up the input parameters of the signal. The output of the device was combined with two branches. The first one was a metal needle immersed in the liquid, in which the SH QCM was immersed, while the second (the ground electrode) was a connection with the surface electrode of the crystal thus creating a droplet/dielectric/electrode capacitive structure. We initially measured the resonance frequency of the SH crystal in air. Then a droplet of water was deposited on the crystal surface and the sensor response was measured again. After that an alternating voltage with step increases of 25 V was applied until a threshold voltage of 100 V was reached, at which a large frequency shift was observed. Subsequently, the voltage was increased with steps of 100 V until it reached the second threshold of 500 V. At this critical value a dielectric breakdown occurred and the experiment was terminated. After each voltage step the crystal was disconnected from the amplifier and connected to an Agilent 8712ET network analyzer. The resonance frequency was recorded and fitted to a BVD model. The experiment was repeated for the three further SH QCMs, but with an upper voltage applied not exceeding 400 V, thus avoiding the dielectric breakdown occurrence.

3. Results and discussions

3.1. Investigation of QCM resonance behaviour in air

Figure 1 a) and b) illustrate the resonance frequency and the resistance shifts of an uncoated 5 MHz QCM against glycerol/water solutions with different concentrations. The dotted lines represent the theoretical values calculated by the Kanazawa and Gordon equation, while the solid lines are the values obtained by the experiment. The frequency and resistance shifts in the range of 0-70% follow the predictions of Kanazawa and Gordon. A slight difference between theory and experiment is observed for concentrations over 70%, which is most likely due to the hygroscopic nature of glycerol, which tends to absorb water molecules from the ambient air and the fact measurements were performed in an open lab.

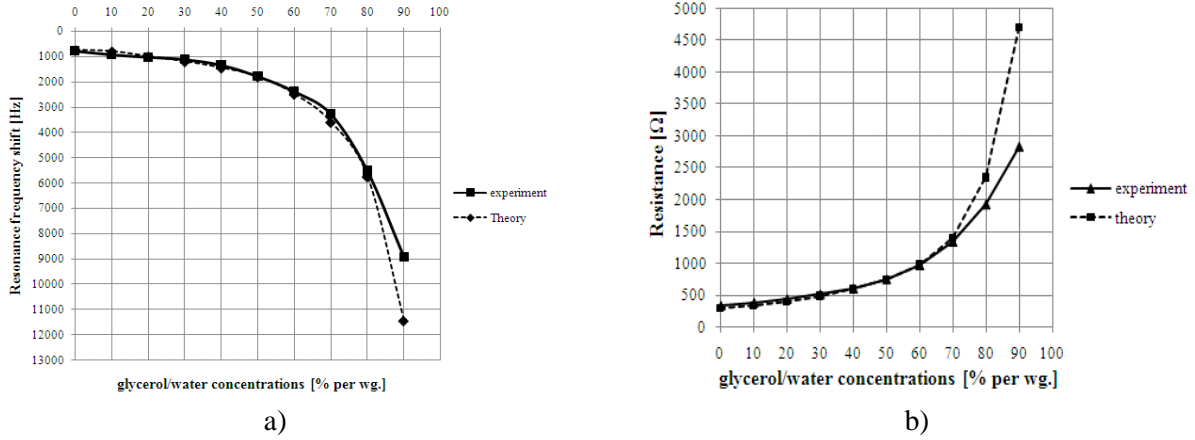


Figure 1: (a) Resonance frequency and (b) resistance of an uncoated QCM operating in glycerol/water solutions with different concentrations.

Table 1 reveals the electrical characteristics of five QCMs, operating in air at the same fundamental frequency of approximately 5 MHz, after the superhydrophobic coating was applied. The deposition of composite epoxy-soot SH layer on the crystal surface leads to a proportional frequency down shift in the range of 64÷90 KHz (12800-18000 ppm), an increase in the bandwidth by an average value of 8.4 KHz and a corresponding increase in the insertion loss of 6.2 dB.

Table 1: Electrical characteristics in air of the QCM prior to and after deposition of epoxy-soot SH layer.

QCM №	QCM status	fr (MHz)	BW (KHz)	Q factor	Insertion losses (dB)	R (Ω)
1	Prior to	5.028655	0.214	23525.5	-7.7	118
	After SH	4.953138	6.199	799.02	-0.77	1130
2	Prior to	5.022336	0.213	23535.6	-6.58	136
	After SH	4.942000	6.197	797.48	-0.72	1210
3	Prior to	5.019909	0.211	23750.8	-6.39	137
	After SH	4.946988	9.5	520.7	-0.54	1600
4	Prior to	5.025575	0.212	23725.7	-8.51	109
	After SH	4.935535	9.5	519.5	-0.55	1600
5	Prior to	5.028312	0.211	23830.9	-5.55	157
	After SH	4.964032	11.84	419.3	-0.425	2025

Figure 2 compares the resonance spectra behavior of QCM with (a) uncoated, (b) epoxy coated and (c) superhydrophobic surface. For the case of an uncoated surface the quartz crystal operates at fundamental frequency of approximately 5 MHz and supports narrow bandwidth of 211 Hz. The deposition of an epoxy resin coating leads to a frequency down shift of 64 kHz and an increase in insertion loss to 3 dB, although the sensor still maintained a narrow bandwidth of 730 Hz; this increase in damping was likely to be caused by the rougher surface of the epoxy compared to the polished crystal surface. The superhydrophobic coating causes a more substantial increase in the level of insertion loss to 8 dB and

increased the bandwidth to 6.19 kHz. This can be interpreted as an additional dissipation of energy in air due to the high level of surface roughnesses [29].

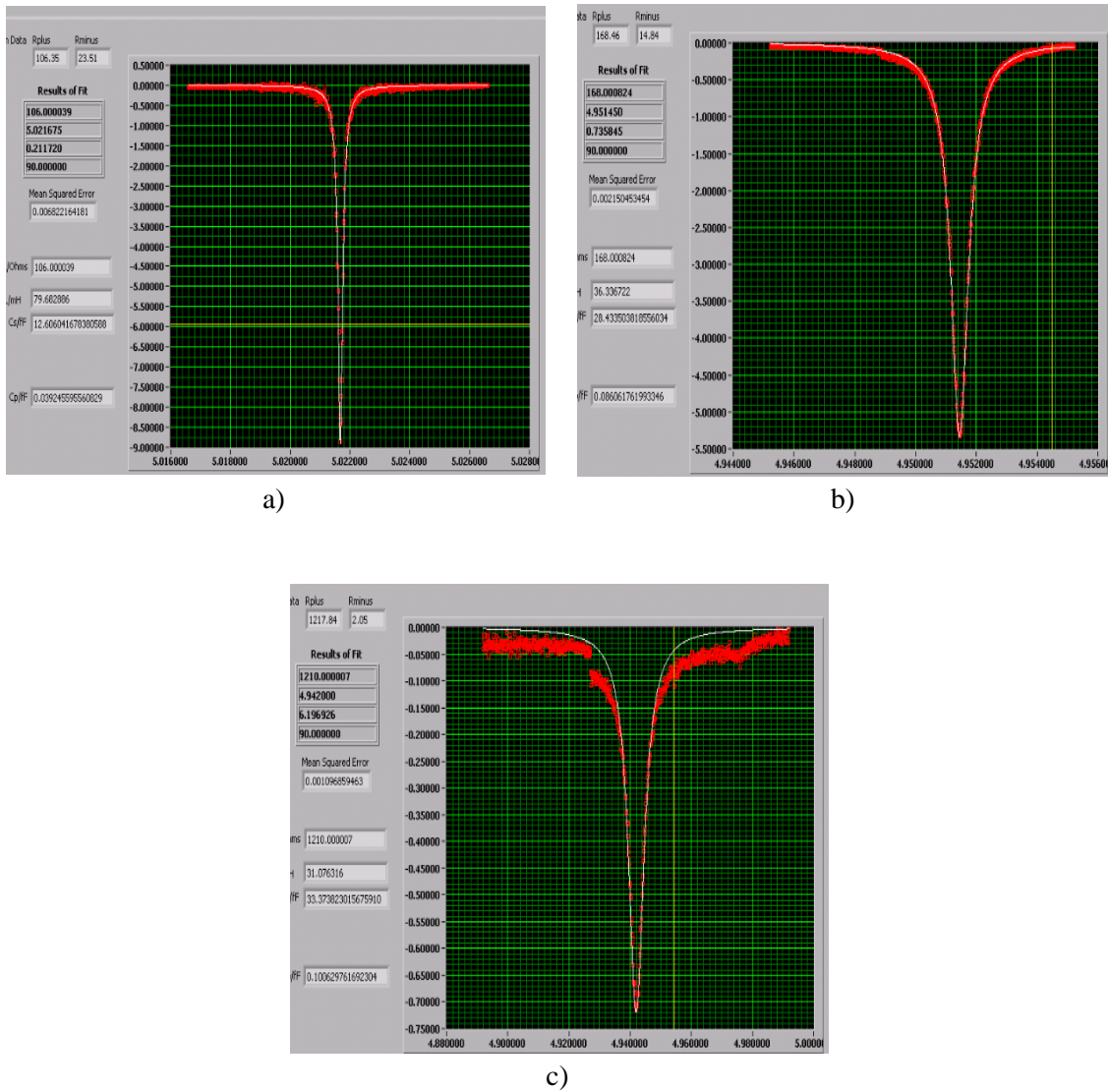


Figure 2: Resonance spectra of a 5 MHz QCM in air with (a) uncoated, (b) epoxy resin coated and (c) SH surface and their fits (white curves) achieved by the BVD fitting model.

All SH coated devices continued to operate with well behaved single mode resonance and good sensitivity. The thickness of the epoxy coating was measured via profilometer Bruker AXS Dektak XT and compared to the value obtained by the theoretical calculation through Sauerbrey's equation using an assumed density of the epoxy resin/hardener mixture, which is $\rho_{ep} = 1.0863 \text{ g/cm}^3$. The experimentally measured thickness was in the range of $9 \pm 0.5 \text{ }\mu\text{m}$, while the theoretical calculations gave a thickness $d \sim 11 \text{ }\mu\text{m}$.

3.2. Wetting state transition triggered using ethanol-water mixtures

Figure 3 shows the resonance frequency shifts of a 5 MHz gold electrode QCM with an uncoated surface versus different aqueous ethanol solutions, obtained by experiment and by theoretical calculation according to the Kanazawa and Gordon equation. The graphical dependence shows that the resonance frequency shifts achieved by experiment and theoretically calculated are in consistence with slight deviation of the experimental data set at some concentrations.

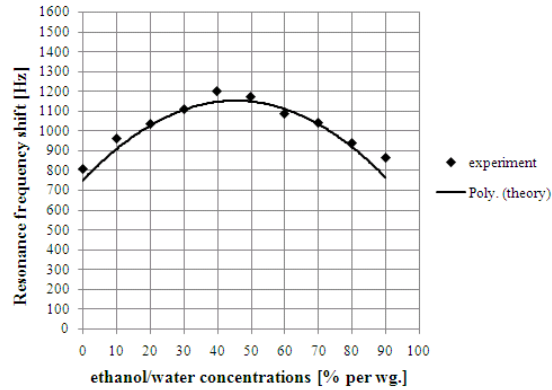


Figure 3: Experimental resonance frequency shift (dotted curve) of 5 MHz QCM with an uncoated surface and its theoretical 2nd order polynomial fit (solid curve) versus % ethanol concentrations in the range of 0 ÷ 90 % per weight.

Since the experiments were performed in an open lab, there was a slight temperature deviation in the range of 20 °C-26 °C, therefore the experimental data were corrected with the pre-factor for the ethanol, which is $8.49 \cdot 10^{-11}$ [cm³/second. molecule]. The resonance spectra of the first SH QCM was observed at % ethanol concentrations in the range of 0-12.5% per weight. For comparison glass microscope slides were also coated with a superhydrophobic epoxy-soot layer and the contact angle variation of droplets with different ethanol concentrations was investigated. The results are summarized in figures 4 and 5. At concentrations between 0 and 10 % the resonance frequency shifts are almost the same and 2.5 times lower compared to these obtained through the QCM with an uncoated surface (see experimental curve in fig. 3). This effect can be attributed to the efficient decoupling of the sensor response achieved by the superhydrophobization of the crystal surface; the same tendency is reported in reference [8]. Also the dissipation factor and the resonance frequency shifts keep approximately constant values in this range of concentrations. Further increase of the ethanol concentration leads to a large 700 Hz frequency down shift of the QCM at 12.5 % concentration of ethanol accompanied by decrease in the dissipation factor at the same concentration. Contact angle measurements show that at this concentration of ethanol on epoxy-soot coated surfaces there is a large contact angle change from 155° to 116°, indicating this is critical concentration at which the surface undergoes a transition from the superhydrophobic Cassie-Baxter state to a more hydrophilic state.

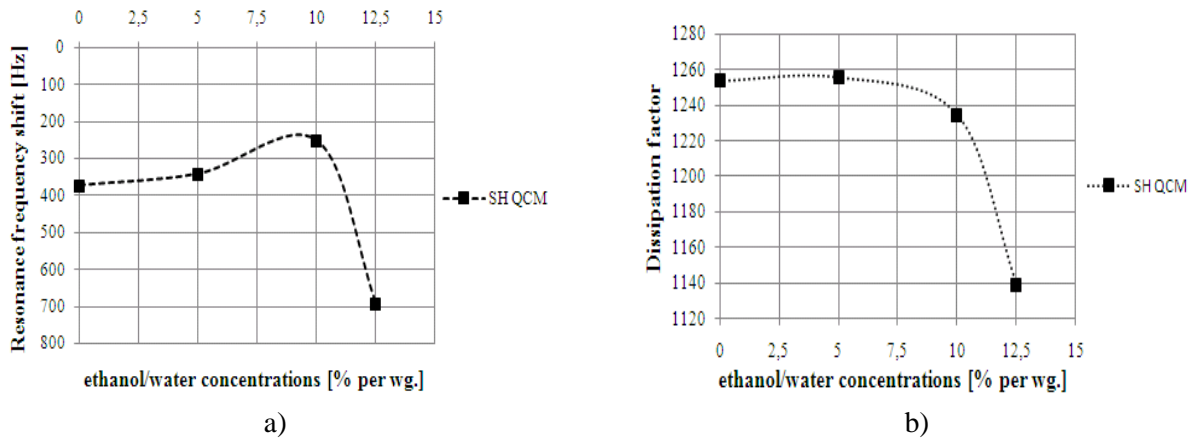


Figure 4: (a) Frequency response and (b) dissipation factor of the SH QCM for % ethanol concentrations in the range of 0÷12.5 % per weight.

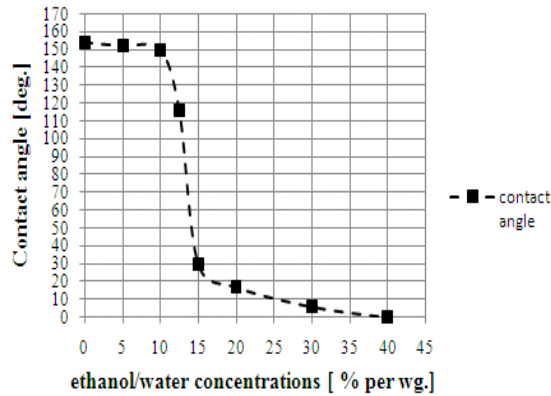


Figure 5: Contact angle variation of droplets of aqueous ethanol solutions on epoxy-soot coated surfaces with different concentrations.

The decrease in dissipation accompanying the decrease in frequency shift and the change to a hydrophilic state suggests the observed transition is not a simple Cassie-Baxter to Wenzel wetting state transition. After removal from the ethanol solution the surface was observed to have a SCA to water of 116° and so was no longer superhydrophobic. Using a hydrophobic chemical treatment a SCA of 152° could be achieved with low contact angle hysteresis of 1.3°. We further examined the quartz crystal surface using a scanning electron microscope (SEM). Figure 6 compares a surface exposed to the ethanol solution and an area of surface not exposed to the ethanol solution. The comparison shows that the peak features are more rounded after exposure to the ethanol. These results suggest that the application of aqueous ethanol solution with 12.5% concentration may cause surface chemical and structural changes.

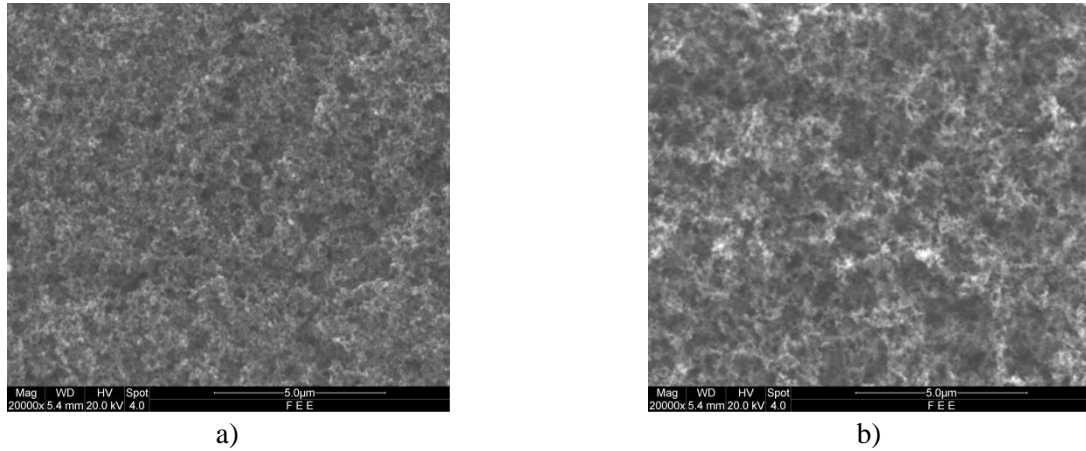


Figure 6: Scanning electron microscopy of (a) the affected and (b) unaffected area of the superhydrophobic QCM.

3.3. Wetting state transition triggered using electrowetting

To achieve a wetting state transition, which on drying the crystal could be reversed, we considered applying a voltage using an electrowetting configuration. The results of the electrical performance of these devices are summarized in table 2.

Table 2: Average electrical characteristics of four SH QCMs during electrowetting.

State of the QCM	Resonance frequency f_r (MHz)	Resistance R (Ω)	Bandwidth BW (kHz)	$\Delta f = f_{\text{air}} - f_{\text{rEW}}$ (Hz)	$D = \text{BW}/f_r$
QCM in air	4.952165	1424.4	8.29	0	$1674 \cdot 10^{-6}$
QCM in water	4.951863	1523.9	8.47	302	$1710 \cdot 10^{-6}$
QCM at 25V	4.951845	1525.1	8.47	320	$1710 \cdot 10^{-6}$
QCM at 50V	4.951820	1529.3	8.46	345	$1708 \cdot 10^{-6}$
QCM at 75V	4.951807	1530.1	8.47	358	$1710 \cdot 10^{-6}$
QCM at 100V	4.951426	1542.4	8.48	739	$1713 \cdot 10^{-6}$
QCM at 200V	4.951425	1546.6	8.49	740	$1715 \cdot 10^{-6}$
QCM at 300V	4.951402	1547.6	8.48	763	$1713 \cdot 10^{-6}$
QCM at 400V	4.951387	1544.6	8.49	778	$1715 \cdot 10^{-6}$

Table 2 shows the electrical characteristics of four SH QCMs during electrowetting presented as average data from eight independent electrowetting measurement cycles. Figure 7 compares (a) the resonance frequency shifts of a SH quartz crystal with that of an epoxy coated QCM, and (b) the contact angle variation at different values of the applied voltage. The inclusion of an epoxy coated QCM as a

comparison device allows us to evaluate whether possible frequency shifts are caused by a transition in the wetting state or by changes, such as in the piezoelectric stiffness. For the SH QCM a step change in frequency is observed at between 75 V and 100 V with little change in dissipation. Above this voltage the frequency decreased only slightly. Moreover, throughout the experiment the dissipation remained broadly constant at the initial value measured on immersion. In our measurements the epoxy layer suffered irreversible damage at a threshold voltage of 500 V. Interestingly, the initial frequency down shift on immersion of the SH QCM in water is only 302 Hz and is 2.5 times lower than the case of a QCM with an uncoated surface (see fig. 1a and fig. 3). We also note that the epoxy coated crystal did not show any significant step changes or variations in the resonance frequency behavior as voltage was increased; the shifts were within 56 Hz. One interpretation of the data is that the superhydrophobic coating decouples the QCM response compared to the uncoated and epoxy coated QCM and that a wetting state transition is detected at between 75 V and 100 V.

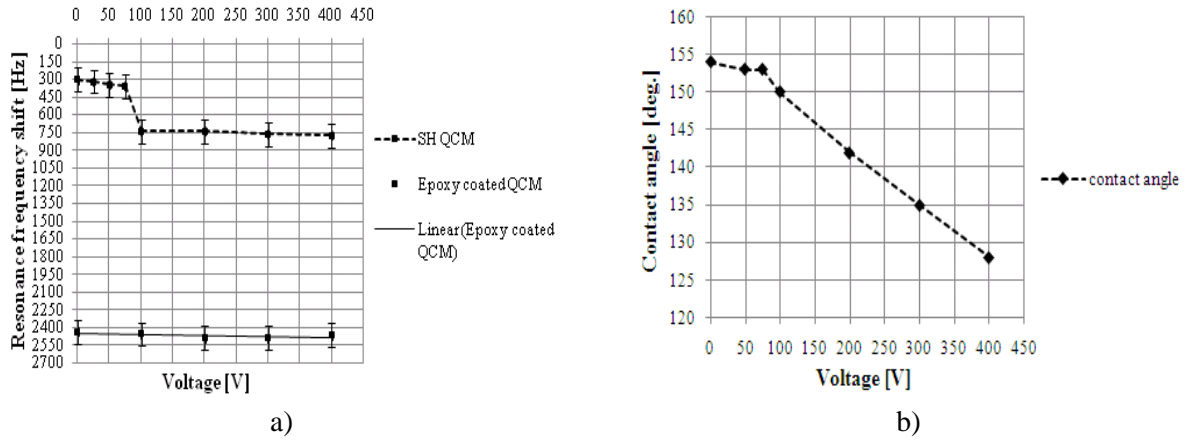


Figure 7: Resonance frequency down shift of (a) a SH and epoxy coated QCMs and (b) contact angle variations of water droplet resting upon gold coated SH glass slide during electrowetting.

To investigate the hypothesis of a wetting state transition, the droplet contact angle behaviour over the same range of voltages was studied. The basic equation for droplet contact angle changes using electrowetting is:

$$\cos\theta = \cos\theta_y + \left(\frac{\epsilon_0\epsilon_d}{2d\gamma_{lv}}\right)V^2 \quad (2),$$

Where $\cos\theta_y$ is the initial contact angle, ϵ_0 is the dielectric permittivity in vacuum, ϵ_d is the dielectric permittivity of the layer, d is its thickness, γ_{lv} is the interfacial energy between liquid and vapor (surface tension) and V is the applied voltage. This relation shows that for a given dielectric layer an applied voltage will reduce the contact angle causing improved wettability. We also know from previous studies that the associated electrocapillary pressure can cause a droplet in a suspended Cassie-Baxter state to collapse into a penetrating Wenzel state [18]. Figure 7 b) reveals the contact angle behavior of a water droplet resting upon gold coated SH glass slide. From 0V to 100 V there are no significant changes in the contact angle but upon passing to 200 V a decrease in the contact angle is observed. Further voltage increase leads to further decrease in the contact angle and for 400 V the contact angle has reduced by 26°. Moreover the CAH also increased and droplet mobility was observed to reduce. To check the chemical

and surface structure had not been altered by electrowetting, crystals were dried after the QCM experiments and static contact angle and contact angle hysteresis measurements performed. Prior to and after electrowetting the SCA was in the range of 151°-155° and the CAH was 1°-3.7° (table 3).

Table 3: Contact angle of four SH QCMs prior to and after electrowetting.

QCM №	CA status	Static CA [°]	Advancing CA [°]	Receding CA [°]	CAH [°]
QCM_2	prior to	152.4	156.7	153	3.7
	after EW	152.0	155.0	152.7	2.3
QCM_3	prior to	155.2	150.3	149.3	1
	after EW	154.6	153.3	151.7	1.6
QCM_4	prior to	152.4	153.0	150.8	2.2
	after EW	151.9	153.4	151.2	2.2
QCM_5	prior to	150.8	156.2	153.4	2.8
	after EW	151.7	153.2	150.8	2.4

4. Conclusions:

In this work we have presented results from systematic experimental investigation on the wetting state response of quartz crystals possessing a superhydrophobic soot-epoxy coating. Possible triggering of wetting state transitions using ethanol solutions and electrowetting has been developed. The first of these methods was found to cause surface changes, but the second method appeared to trigger a wetting state transition without surface damage. This wetting state transition appears to be observable as an electrowetting induced frequency down shift of 778 Hz. The transition voltage is consistent with droplet contact angle decreases on similar surfaces. The step change in frequency was not accompanied by any significant change in the QCM dissipation. The proof-of-concept that an acoustic wave signal change, here a quartz crystal resonance frequency, can be observed when a superhydrophobic surface wetting state change is triggered, may provide an additional sensor mechanism to the usual mass or viscosity-density induced changes. The optimization of such superhydrophobic coated sensors may allow the development of a new acoustic wave based sensor with controllable wettability for detecting changes in hydrophobicity of surfaces.

Acknowledgements: The authors wish to gratefully acknowledge Dr. Guillaume Zoppi and Mr. Pietro Maiello from the University of Northumbria at Newcastle (UK) for the assistance with the laboratory equipment. KE also thanks the EU for financial support under its Erasmus Exchange programme.

References:

- [1] Sauerbrey G 1959 *Physics* **155** 206-222
- [2] Nomura T and Okuhara M 1982 *Anal. Chem.* **142** 281-284
- [3] Buttry D 1991 *Electroanal. Chem.* **17** 1-86

- [4] Muratsugu M, Ohia F, Miya Y, Hosokawa T, Kurosawa S, Kamo N and Ikeda H 1993 *Anal. Chem.* **65** 2933-2937
- [5] Kanazawa K and Gordon J 1985 *Anal. Chem.* **57** 1770-1772
- [6] Bruckenstein S and Shay M 1985 *Electrochimica Acta* **30** 1295-1300
- [7] Shirtcliffe N, McHale G, Atherton S and Newton M 2010 *Elsevier* **161** 124-138
- [8] Quere D, Lafuma A and Bico J 2003 *Nanotechn.* **14** 1109-1112
- [9] Roach P, McHale G, Evans C, Shirtcliffe N and Newton M 2007 *Langmuir* **23** 9823-9830
- [10] Evans C, McHale G and Shirtcliffe N 2005 *Sens. and Act. A-Phys.* **123-24** 73-76
- [11] Fujita M, Muramatsu H and Fujihira M 2005 *Japan. Jour. of appl. Phys. part 1* **44** 6726-6730
- [12] Kwoun SJ, Lee R, Cairncross R, Shah P and Brinker C 2006 *IEEE TUFFC* **53** 1400-1403
- [13] Thompson M, McHale G and Newton M 2005 *Can. patent appl.* CA2451413
- [14] Shirtcliffe N, McHale G, Newton M, Perry C and Roach P 2005 *Chem. Com.* **25** 3135-3137
- [15] Shirtcliffe N, McHale G, Newton M, Perry C and Roach P 2007 *Mater. Chem. and Phys.* **103** 112-117
- [16] Verplanck N, Coffinier Y, Thomy V and Boukherroub R 2007 *Nanoscale Res. Lett.* **2** 577-596
- [17] Mugele F, Baret J 2005 *Jour. of Phys. Cond. Matt.* **17** 705-774
- [18] Herbertson D, Evans C, Shirtcliffe N, McHale G and Newton M 2006 *Sens. and Act. A-phys.* **130-131** 189-193
- [19] McHale G, Roach P, Evans C, Shirtcliffe N, Elliot S and Newton M 2008 *IEEE Freq. Cont. Symp.* 698-704
- [20] Zhang X, Shi F, Niu J, Jiang Y and Wang Z 2008 *Mater. Chem.* **18** 621-633
- [21] Levkin P, Svec F and Frechet 2009 *Adv. Func. Mater.* **19** 1993-1998
- [22] Qu M, He J and Cao B 2010 *Appl. Surf. Sci.* **257** 6-9
- [23] Deng X, Mammen L, Butt H and Volmer D 2012 *Science* **335** 67-70
- [24] Yuan L *et al* 2011 *Acs. Nano* **5** 4007-4013
- [25] Lotters J, Olthuis W, Veltink P and Bergveld P 1997 *Micromech. Microeng.* **7** 145-147
- [26] Brostow W and Glass N 2003 *Mater. Res. Innov.* **7** 125-132
- [27] Roach P, Shirtcliffe N and Newton M 2008 *Soft Matter* **4** 224-240

[28] King M 1981 *Austr. Jour. of Soil Res.* **19** 275-285

[29] Wu S, Shi L, Garfield L, Tabor R, Striolo A and Grady B 2011 *Langmuir* **27** 6091-6098